Current Optics and Photonics
Vol. 2, No. 6, December 2018, pp. 576-581

ISSN: 2508-7266(Print) / ISSN: 2508-7274(Online)
DOI: https://doi.org/10.3807/COPP.2018.2.6.576

Approach for Microwave Frequency Measurement Based on a Single Photonic Chip Combined with a Phase Modulator and Microring Resonator

Jiahong Zhang*, Chuyi Zhu, Xiumei Yang, Yingna Li, Zhengang Zhao, and Chuan Li

Faculty of Information Engineering and Automation, Kunming University of Science and Technology, Kunming 650504, China

(Received August 8, 2018 : revised October 11, 2018 : accepted November 4, 2018)

A new approach for identification of a microwave frequency using an integrated optical waveguide chip, combined with a phase modulator (PM) and two microring resonators (MRRs), is proposed, theoretically deduced, and verified. By wavelength tuning to set the PM under the condition of a double side band (DSB), the measurement range can be started from the dc component, and the measurement range and response slope can be adjusted by designing the radius and transmission coefficient of the MRR. Simulations reveal that the amplitude comparison function (ACF) has a monotonic relationship from dc to 32.5 GHz, with a response slope of 5.15 dB under conditions of DSB modulation, when the radius values, transmission coefficients, and the loss factors are designed respectively as R_1 = 400 μm, R_2 = 600 μm, $t_1 = t_2$ = 0.63, and $\gamma_1 = \gamma_2$ = 0.66. Theoretical calculations and simulation results both indicate that this new approach has the potential to be used for measuring microwave frequencies, with the advantages of compact structure and superior reconfigurability.

Keywords : Microwave photonics, Frequency measurement, Photonic integrated circuits, Micro-ring resonator (MRR)
OCIS codes : (130.0130) Integrated optics; (130.3120) Integrated optics devices; (230.7370) Waveguides; (350.4010) Microwaves

I. INTRODUCTION

Microwave frequency identification has been extensively researched and widely used in the areas of biomedicine, communications, electronic countermeasures (ECM), radar warning, etc [1]. For this purpose, instantaneous frequency measurement (IFM) techniques are required to determine the frequency of incoming microwave signals with large instantaneous frequencies (up to tens of GHz) and wide bandwidth (from MHz to hundreds of GHz). As is known, due to frequency sweeping the real-time bandwidth of traditional, purely electronic frequency-measurement systems is limited to no more than 1 GHz [2]. To address the challenges of traditional electronic solutions, photonic-based IFM techniques have been proposed and researched, thanks to the inherently broad band width, wider frequency coverage, lighter weight, smaller footprint, low frequency-dependent loss, and strong immunity to electromagnetic interference (EMI) [3-6]. However, most of these demonstrated photonic-assisted IFM approaches are mainly based on bulky and expensive off-the-shelf discrete optical components, such as optical modulators, filters, and polarization controllers, therefore penalizing the overall system stability, compactness, and unit cost. To overcome the aforementioned problems, several IFM systems based on integrated optics have been reported recently, but these systems require high optical power (4.1 W) to enable nonlinear optical processing, and also demand an independent optical phase modulator (PM), which increases system size and cost [7-10].

In this paper, an IFM approach based on an integrated optical waveguide chip, combined with two optical filters and an optical PM, is proposed, designed, and analyzed, to address the compactness and power issues of current

*Corresponding author: zjh_mit@163.com, ORCID 0000-0003-1496-5770
Color versions of one or more of the figures in this paper are available online.

integrated optical solutions. Because only one optical laser, one integrated optical waveguide chip, and two low-frequency PDs are used to acquire the amplitude comparison function (ACF), the cost and size of the measurement system are reduced effectively.

II. METHODS

The diagram of the proposed microwave frequency-measurement approach is schematically shown in Fig. 1.

As can be seen, an integrated optical waveguide Y branch incorporated with a modulation electrode between the input straight arm and two optical waveguide rings of different radii, along with the two output arms, are designed and fabricated on the same substrate chip. As a result, both an optical PM and two microring resonators (filters) are formed on a single photonic chip. The microwave signal under measurement is loaded onto the optical carrier by the PM, while the two MRRs are used as optical filters with different responses, to transform the phase modulation to intensity modulation (PM-IM). The linearly polarized light beam output from the tunable laser travels through polarization-maintaining fiber (PMF) to connect to the integrated photonic chip, and two single-mode fibers (SMF) are used to transmit the two output optical signals to the two low-frequency photodetectors (PDs) for photoelectric conversion. Finally, using a digital signal processing (DSP) unit, the ACF is calculated, and the unknown frequencies are identified.

As is known, the PM output modulated optical field can be expressed as

$$E(t) = \sqrt{P_0}\, e^{j[\omega_c t + m\cos(\omega_m t)]} = \sqrt{P_0}\, e^{j\omega_c t} \sum_{n=-\infty}^{\infty} j^n J_n(m) e^{jn\omega_m t} \quad (1)$$

where P_0 and ω_c are the power and frequency of the input optical signal respectively, $J_n(.)$ denotes a Bessel function of the first kind of order n, $m = \pi(V_m/V_\pi)$ is the phase-modulation index, and V_m and ω_m are the amplitude and frequency of the microwave signal being measured.

Mathematically, under small-signal conditions, the output high-order side bands of the PM can be neglected, so that the output spectrum consists of only the optical carrier and the two first-order side bands:

$$E(t) = \sqrt{P_0}\{J_0(m)e^{j(\omega_c t)} + J_1(m)e^{j[(\omega_c-\omega_m)t+\frac{\pi}{2}]} + J_1(m)e^{j[(\omega_c+\omega_m)t+\frac{\pi}{2}]}\} \quad (2)$$

According to Eq. (2), the first two side bands of the PM have essentially equal amplitudes but opposite phases; hence the output electrical signal from the square-law photodetector (PD) has only a dc component, which means the unknown frequency cannot be extracted under such conditions. To attain PM-IM conversion as shown in Fig. 1, two optical waveguide MRRs are designed as optical filters to break the phase and amplitude relations between the side bands. The responses of the two MRRs can be written as [11]

$$H_k(\omega) = \frac{t_k^2 + \gamma_k^2 - 2t_k\gamma_k\cos\varphi_k}{1 + t_k^2\gamma_k^2 - 2t_k\gamma_k\cos\varphi_k} \quad (3)$$

where k = 1 or 2, corresponding to the up or down optical MRR. $\varphi_k = 4\pi^2 R_k n/\lambda$ is the optical phase difference in the microring, n is the effective refractive index of the optical waveguide, R_k and γ_k are the radius and loss factor of the ring cavity respectively, and t_k is the transmission coefficient between the microring and the straight waveguide arm.

According to the responses of the two MRRs, by wavelength tuning the PM can be set to the four different modulation conditions of DSB, OSC, USB, and LSB, as shown in Fig. 2. Therefore, each output frequency component is multiplied by a different frequency weight of $H_k(\omega)$, and the output optical fields are described as

$$E(\omega) = \begin{cases} 2\pi\sqrt{P_0/2}[J_0(m)H_k(\omega_c) + jJ_1(m)H_k(\omega_c-\omega_m) + jJ_1(m)H_k(\omega_c+\omega_m)] \\ 2\pi\sqrt{P_0/2}[jJ_1(m)H_k(\omega_c-\omega_m) + jJ_1(m)H_k(\omega_c+\omega_m)] \\ 2\pi\sqrt{P_0/2}[J_0(m)H_k(\omega_c) + jJ_1(m)H_k(\omega_c+\omega_m)] \\ 2\pi\sqrt{P_0/2}[J_0(m)H_k(\omega_c) + jJ_1(m)H_k(\omega_c-\omega_m)] \end{cases} \quad (4)$$

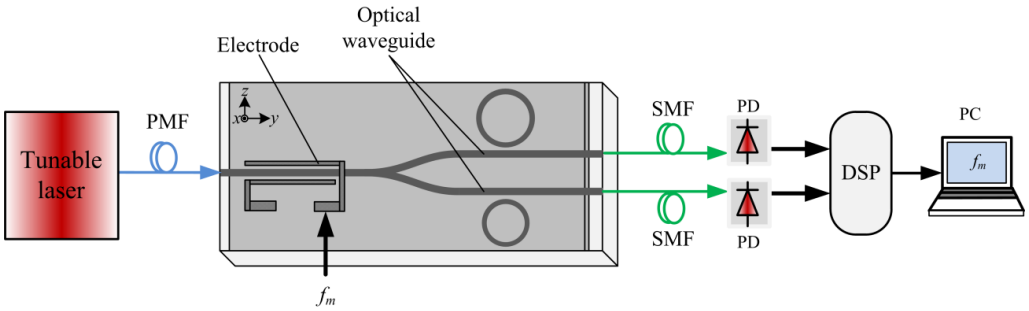

FIG. 1. Schematic diagram of the proposed IFM approach: f_m, the microwave frequency to be measured; PMF, polarization maintaining fiber; SMF, single mode fiber; PD, photodetector; PC, personal computer.

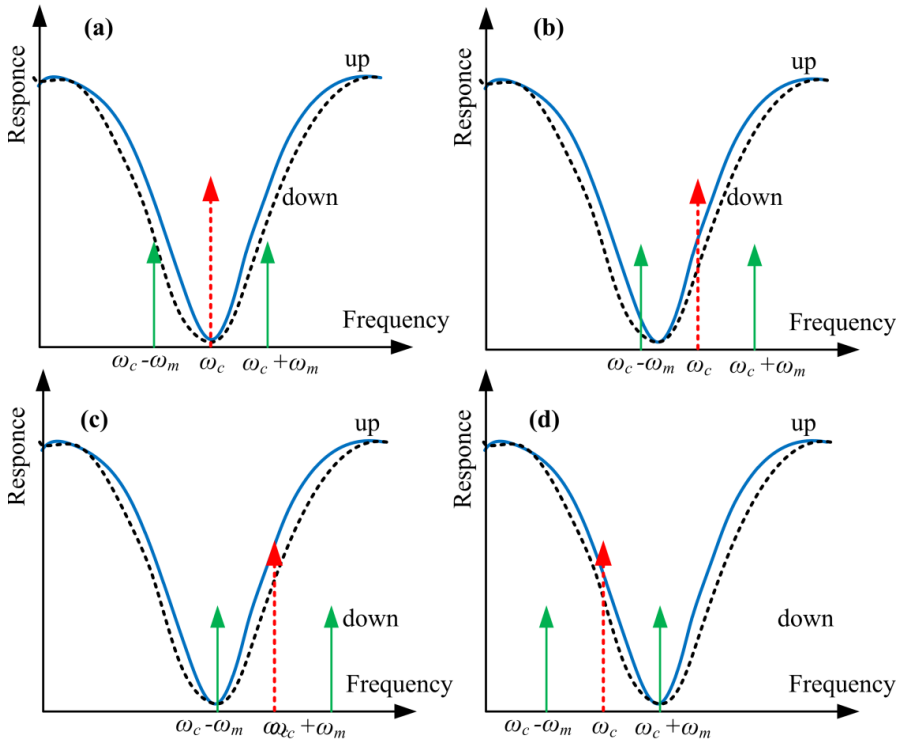

FIG. 2. Response of the two photonic MRRs, under the four modulation conditions: (a) optical carrier suppression (OCS), (b) double side band (DSB), (c) upper side band (USB), (d) lower side band (LSB).

According to Eq. (4), by using the square-law PD and neglecting the $J_n(.)^2$ terms, the alternating current (ac) can be obtained as

$$i_{AC,k}(\omega) \propto \begin{cases} 2\pi^2 P_0[jJ_0(m)J_1(m)H_k(\omega_c)H_k(\omega_c-\omega_m)+jJ_0(m)J_1(m)H_k(\omega_c)H_k(\omega_c+\omega_m)] \\ 2\pi^2 P_0[-J_1^2(m)H_k(\omega_c-\omega_m)H_k(\omega_c+\omega_m)] \\ 2\pi^2 P_0[jJ_0(m)J_1(m)H_k(\omega_c)H_k(\omega_c+\omega_m)] \\ 2\pi^2 P_0[jJ_0(m)J_1(m)H_k(\omega_c)H_k(\omega_c-\omega_m)] \end{cases} \tag{5}$$

Based on Eq. (5), the amplitude comparison function (ACF) between the two detected ac components is expressed as

$$\mathrm{ACF}(\omega_m) = \begin{cases} \dfrac{H_1(\omega_c)[H_1(\omega_c-\omega_m)+H_1(\omega_c+\omega_m)]}{H_2(\omega_c)[H_2(\omega_c-\omega_m)+H_2(\omega_c+\omega_m)]} \\ \dfrac{H_1(\omega_c-\omega_m)H_1(\omega_c+\omega_m)}{H_2(\omega_c-\omega_m)H_2(\omega_c+\omega_m)} \\ \dfrac{H_1(\omega_c)H_1(\omega_c+\omega_m)}{H_2(\omega_c)H_2(\omega_c+\omega_m)} \\ \dfrac{H_1(\omega_c)H_1(\omega_c-\omega_m)}{H_2(\omega_c)H_2(\omega_c-\omega_m)} \end{cases} \tag{6}$$

From Eq. (6), the ACF can be calculated by the response of the two MRRs, which depends neither on the laser output power nor the microwave modulation index, but only on the microwave frequency being measured. The ACF exhibits a monotonic relationship to the unknown microwave frequency, which means the frequency can be estimated from the measured ACF value. Besides, to ensure that the ACF exhibits a monotonic relationship to the measured frequency, the two MRRs must have the same resonant frequency, by wavelength tuning, because if the two MRRs have resonant-frequency mismatch (working under different modulation conditions), the $J_n(m)$ term remains in the expression for ACF, which means the ACF has a relationship to both the frequency and amplitude of the measured microwave signal, such that the frequency cannot be measured.

III. RESULTS

To highlight the configurability, based on the theory above and considering the current level of fabrication technology for a $LiNbO_3$ waveguide, two integrated optical waveguide MRRs are designed with radii of R_1 = 400 μm and R_2 = 600 μm, loss factors of $\gamma_1 = \gamma_2$ = 0.66, and different transmission coefficients of 0.63 and 0.75. The responses are shown in Figs. 3(a) and 3(b). It can be seen that the extinction ratios (ER) are 24.98 dB and 14.47 dB respectively for the two MRRs with transmission coefficients of 0.63 and 0.75. Besides, the modulation conditions can be set to OCS, DSB, USB, and LSB respectively when the output wavelengths of the tunable laser are tuned to 1549. 875, 1549.9, 1549. 975, and 1549.775 nm.

However, one of the strongest determinants for MRR design is the current waveguide-fabrication technology, which is mainly related to the adopted waveguide material. For example, as the loss factor of a silicon or polymer waveguide is smaller, the radius of the MRR can be designed smaller than those in this paper. Consequently, to design the MRR, practical requirements, current fabrication technology, adopted waveguide material, and simulation results should all be take into account.

Furthermore, according to Eq. (6) and using the results shown in Fig. 3, the responses of the two MRRs together with the ACF under the four modulation conditions OSC, DSB, USB, and LSB are shown in Figs. 4(a), 4(b), 4(c), and 4(d) respectively, in which as an example the modulation

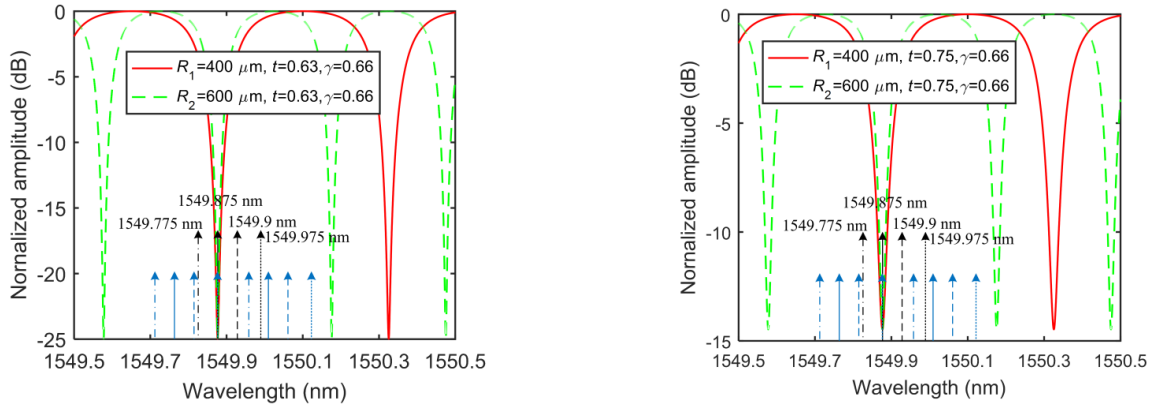

FIG. 3. Response of the designed MRRs for (a) $t = 0.63$ and (b) $t = 0.75$.

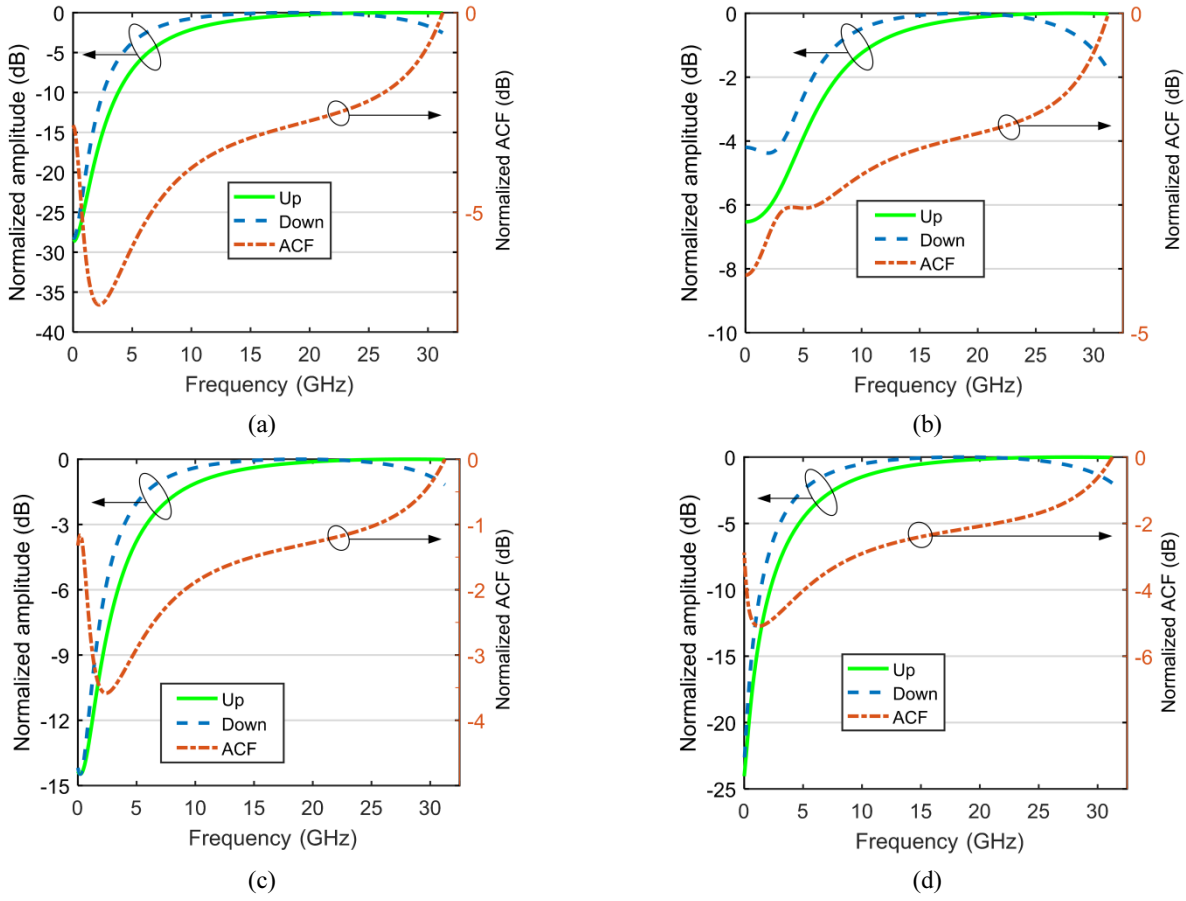

FIG. 4. MRR frequency responses together with the ACF, under modulation conditions of (a) OCS, (b) DSB, (c) USB, and (d) LSB.

frequency is set at 12.5 GHz. As can be seen in Fig. 4, the ACF is monotonic over the entire frequency range from dc to 32.5 GHz, with a response slope of 5.19 dB under DSB modulation. However, the monotonic ACF ranges are only 19.63~32.5 GHz, 20.84~32.5 GHz, and 9.41~32.5 GHz respectively under modulation conditions of OSC, USB, and LSB, with response slopes of 2.74, 1.82, and 3.00 dB. The reason why DSB modulation yields the best results, under certain geometric conditions at least, comes from two main sides. One is that, under DSB modulation, the carrier frequency ω_c and the two side bands $\omega_c+\omega_m$ and $\omega_c-\omega_m$ are all included; as a result, the frequencies from $-\omega_m$ to $+\omega_m$ are generated through the differentiation operation, which means the measurement range can start with dc. The other is from the viewpoint of energy: under DSB modulation, as the two side bands are included the power of the measured microwave signal is larger, and hence the signal-to-noise ratio is higher.

As a comparison, another ACF is calculated when the transmission coefficients of the two MRRs are chosen to be 0.75 and the other parameter values are kept unchanged. The results are shown in Table 1. It can be seen that the monotonic ACF ranges and response slopes do not exhibit clear changes under modulation conditions of OSC, USB, and LSB. However, the response slope is only 4.01 dB under DSB modulation, which is lower than that for the measurement approach when the transmission coefficient of the MRRs is 0.66. As a result, a larger response slope can be achieved through designing smaller transmission coefficient of the MRRs. Besides, it has to be stated that the measurement range is decided by the free spectral range (FSR = $c/(2\pi nR)$, where c is the speed of light in vacuum) of the MRRs, which can be changed by designing a different radius. In fact, the MRR in this frequency-measurement system is used as the optical filter; therefore, its performance is determined by its radius, transmission coefficient, and loss factor, and in turn the measurement performance is influenced by these parameters. For example, to achieve a larger measurement range, a smaller radius is designed to enlarge the FSR of the MRR, and to achieve a larger response slope, the transmission coefficient is designed to be smaller, to decrease the full width at half maximum (FWHM).

IV. CONCLUSION

An integrated optical waveguide PM combined with two optical waveguide MRRs on a single chip is proposed for the identification of a microwave frequency. Considering previous optical techniques for measuring microwave frequencies using some discrete components, including electro-optic modulators, optical filters, etc., system complexity is increased while stability is decreased. Besides, as the overall system performance is dependent on characteristics of all of the included components, the measurement system is difficult to control. On the other hand, to improve system performance, high-performance electro-optic modulators and optical filters are required, and in turn the price greatly increases. However, in the scheme proposed here, the PM combined with two microring resonators (MRRs) is fabricated on a single chip; therefore the system's complexity is decreased, while its stability and controllability are increased.

The ACF of the proposed IFM system under the four modulation conditions of OCS, DSB, USB, and LSB is theoretically deduced. The theory is supported and verified by simulation results, which reveal that the ACF is monotonic over a large frequency range from dc to 32.5 GHz, and the response slope is 5.15 dB under DSB conditions, when the radii, transmission coefficients, and loss factors are designed respectively as R_1 = 400 μm, R_2 = 600 μm, $t_1 = t_2$ = 0.63, and $\gamma_1 = \gamma_2$ = 0.66. The measurement range and ACF response slope can be changed by designing different transmission coefficient and radius of the MRRs, or by wavelength tuning (changing the PM conditions). All of the results indicate that such an approach has the potential to be used for microwave frequency measurement.

TABLE 1. Simulation results for the proposed IFM approach

Parameters of the designed MRRs	Modulation conditions	Up response slope (dB)	Down response slope (dB)	Measurement range (GHz)	ACF response slope (dB)
R_1 = 400 μm, R_2 = 600 μm, t = 0.63, γ = 0.66	Optical carrier suppression (OSC)	28.68	28.38	19.63~32.5	2.74
	Double side band (DSB)	8.50	5.62	0~32.5	5.19
	Upper side band (USB)	24.98	24.98	20.84~32.5	1.82
	Lower side band (LSB)	23.83	22.92	9.41~32.5	3.00
R_1 = 400 μm, R_2 = 600 μm, t = 0.75, γ = 0.66	Optical carrier suppression (OSC)	28.68	28.36	16.13~32.5	3.01
	Double side band (DSB)	6.53	4.37	0~32.5	4.01
	Upper side band (USB)	14.46	14.47	20.53~32.5	1.23
	Lower side band (LSB)	23.61	22.73	8.7~32.5	3.11

ACKNOWLEDGMENT

This study was supported by the National Natural Science Foundation of China (Grant No. 61765009), the Applied Basic Research Project of Yunnan province (Grant No. 2018FB106), the Introducing Talent Research Start-up Project of KMUST (Grant No.KKSY201603042), and the Scientific Research Foundation Project of Yunnan Education Department (Grant No. 2017ZZX149).

REFERENCES

1. J. B. Tsui, *Microwave Receivers With Electronic Warfare Application* (Wiley Press, New York, USA, 2000).
2. G. Gratton and A. Basu, *An Introduction to Microwave Measurements* (CRC Press, Boca Raton, USA, 2015).
3. H. Zhang and S. Pan, "High resolution microwave frequency measurement using a dual-parallel Mach-Zehnder modulator," IEEE Microw. Compon. Lett. **23**, 623-625 (2013).
4. X. Li, A. Wen, X. Ma, W. Chen, Y. Gao, and W. Zhang, "Photonic microwave frequency measurement with a tunable range based on a dual-polarization modulator," Appl. Opt. **55**, 8727 (2016).
5. Z. Tu, A. Wen, Y. Gao, W. Chen, Z. Peng, and M. Chen, "A photonic technique for instantaneous microwave frequency measurement utilizing a phase modulator," IEEE Photon. Technol. Lett. **28**, 2795-2798 (2016).
6. Y. Ma, D. Liang, D. Peng, Z. Zhang, Y. Zhang, and S. Zhang, "Broadband high-resolution microwave frequency measurement based on low-speed photonic analog-to-digital converters," Opt. Express **25**, 2355 (2017).
7. D. Marpaung, "On-chip photonic-assisted instantaneous microwave frequency measurement system," IEEE Photon. Technol. Lett. **25**, 837-840 (2013).
8. J. S. Fandino and P. Munoz, "Photonics-based microwave frequency measurement using a double-sideband suppressed-carrier modulation and an InP integrated ring-assisted Mach-Zehnder interferometer filter," Opt. Lett. **38**, 4316-4319 (2013).
9. H. Jiang, "Wide-range, high-precision multiple microwave frequency measurement using a chip-based photonic Brillouin filter," Optica **3**, 30-34 (2016).
10. L. Liu, F. Jiang, S. Yan, S. Min, M. He, D. Gao, and J. Dong, "Photonic measurement of microwave frequency using a silicon microdisk resonator," Opt. Commun. **335**, 266-270 (2015).
11. C. K. Madsen and J. H. Zhao, *Optical Filter Design and Analysis* (Wiley, New York, USA, 1999).